



Determination of the Internal Ballistic Properties of Solid Heterogeneous Rocket Propellants

Bogdan FLORCZAK^{1,*}, Marek BIAŁEK², Andrzej CHOLEWIAK²

¹ Institute of Industrial Organic Chemistry,
6 Annopol St., 03-236 Warsaw, Poland

² ZPS „GAMRAT” Sp. z o. o., Jasło, Poland

*E-mail: florczak@ipo.waw.pl

Abstract: This paper describes the determination of the internal ballistic properties of tubular, solid heterogeneous rocket propellant (SHRP) charges based on hydroxyl terminated polybutadiene (HTPB) binder. The SHRP charges were screened (inhibited) on their external cylindrical surfaces and inserted into a laboratory rocket motor (LRM). These determinations originated from theoretical considerations and were developed using experimental measurements from static firings of SHRP charges in an LRM. Due to the design of the SHRP charge, its burning process began from the inner cylindrical surface and from both ends of the ring surfaces. The initial temperatures (T_p) of the SHRP charges tested were 233, 288 or 323 K in single static firing runs. On the basis of the pressure (p) of the combustion products of the SHRP vs. time (t) of the LRM operation, the dependence of the burning rates (r_b) of the SHRP charges on (p) and on (T_p), and also the (r_b) sensitivity to changes in (p) and (T_p), were determined by means of the indirect method.

Keywords: solid heterogeneous rocket propellant (SHRP), internal ballistic properties, laboratory rocket motor (LRM)

1 Introduction

Using a laboratory rocket motor (LRM), it is possible to determine the important internal ballistic parameters of solid heterogeneous rocket propellant (SHRP) charges inserted into the combustion chamber of an LRM, such as the dependence of the burning rate (r_b) on the pressure (p) of the combustion products and on the initial temperature (T_p) of the propellant charge.

Under stationary conditions of the burning process, $r_b(p, T_p)$ is characterized by the following parameters: exponent factor $n(p, T_p) \equiv (\partial \ln r_b / \partial \ln p)_{T_p}$, describing the sensitivity of (r_b) to pressure (p) changes, and $\sigma_p(p, T_p) \equiv (\partial \ln r_b / \partial T_p)_p$, K^{-1} , describing the sensitivity of (r_b) to (T_p) of the propulsive system SHRP-LMR just before firing.

For the entire range of changes in (p) and (T_p), $\sigma_p > 0$, whilst (n) for the SHRP charge itself may have positive, negative, or zero values in different pressure ranges [1]. For a relatively narrow range of (p) and (T_p), it can be assumed that $n \approx \text{constant}$, σ_p does not depend on (T_p) and is only a function of pressure, *i.e.* $\sigma_p = \sigma_p(p)$. Under such circumstances:

$$r_b = ap^n = a_1 \cdot \exp[\sigma_p (T_p - T_{\text{ref}})] p^n \quad (1)$$

where: $a = a_1 \exp[\sigma_p (T_p - T_{\text{ref}})]$ is a pre-exponential factor, and T_{ref} is the reference initial temperature of the propellant charge. For a given SHRP-LRM configuration and T_p , it is possible to determine the a , a_1 and n values. Another ballistic parameter, the pressure sensitivity (π_k) to (T_p), is defined as follows:

$$\pi_k = (\partial \ln p / \partial T_p)_{Kn} \quad (2)$$

where:

$$Kn = S_b / A_t,$$

S_b – (total) burning surface of the propellant charge,

A_t – critical section area of the LRM nozzle.

When π_k and n are known, it is possible to determine σ_p because:

$$\pi_k = \sigma_p / (1 - n) \quad (3)$$

Dependence $r_b(p, T_p)$ is determined experimentally on the basis of the results of the burning of the tested solid rocket propellant charge in the LMR combustion chamber under constant pressure. The method for the indirect determination of parameters such as (n), σ_p and π_k , is the testing method in which an LRM [2-6] or a scaled-down solid rocket motor (SRM) are used [7]. In the present work, the indirect method was employed for the testing of tubular SHRP charges based on hydroxyl terminated polybutadiene (HTPB) binder, screened with an inhibition layer on their external cylindrical surfaces, and using an LRM of original design described in a Polish Patent [8].

Due to the use of the indirect method, it was assumed that the isotropic propellant burning was in an equilibrium state, that the gas pressure and its flow

velocity were constant along the entire LRM, that the gas was a ideal gas and that there was no heat loss. According to the above method, it is possible to determine (r_b) of the tested SHRP charge in the LRM combustion chamber from a plot of (p) versus time (t). In order to determine the above mentioned parameters, it is necessary to measure the following: the thickness of the combustible layer of the propellant charge (web thickness, w_b), the characteristic times of the burning process and its characteristic pressures.

The dimensions of the tested propellant charges without a screening (inhibiting) layer, *i.e.* length (l), outer radius (R), inner radius (r) were: 102, 31, and 15 mm respectively, so the resultant combustible (w_b) (in the radial direction) was 16 mm.

The theoretical (model) tubular propellant charge burning area (S_b) is dependent upon its temporal burnt web thickness (w_x) and also upon the volume (V_b) changes of the burnt part of the propellant charge as a function of (w_x), assuming that the burning process commences simultaneously from the inside of the cylindrical propellant charge surface and from both its heading ring ends, and is described in accordance with the following formulae (4, 5):

$$S_b(w_x) = 2\pi(r + w_x)(1 - 2w_x) + 2\pi[R^2 - (r + w_x)^2] \quad (4)$$

$$V_b(w_x) = \pi(2r + w_x)(1 - 2w_x)w_x + 2\pi(R^2 - r^2)w_x \quad (5)$$

The theoretical changes in (S_b) of a propellant charge with the above described geometry and an inhibition pattern as a function of (w_x), is shown in Figure 1.

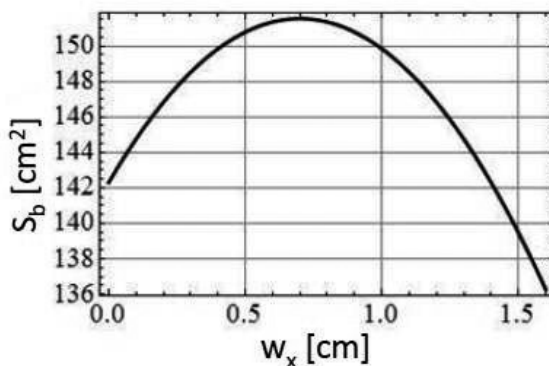


Figure 1. Upper, enlarged part of the theoretical curve describing changes in the burning area (S_b) of a tubular propellant charge of the stated dimensions, inhibited only on the external surface, vs. the burnt temporal web thickness (w_x) of the propellant charge.

The theoretical changes in (V_b) of the propellant charge of the stated geometry and inhibition pattern, as a function of (w_x), is presented in Figure 2.

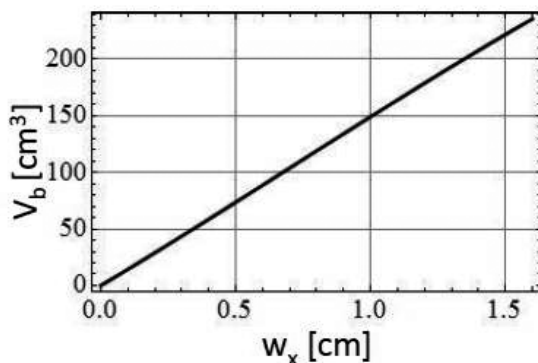


Figure 2. The change in burnt propellant charge volume (V_b) as a function of the burnt temporal propellant charge web thickness (w_x).

Taking into consideration the full scale of the vertical axis (S_b) shown in Figure 1, it can be concluded that the course of the theoretical (S_b) curve during combustion of the above tubular propellant charge is quite flattened, which should result in small fluctuations in the pressure of the combustion products during the burning of the propellant charge inserted in the LRM.

Linear changes in (V_b) during the burning process of the tested tubular propellant charge of the above design (Figure 2) describe a stable process of propellant charge consumption (stable mass regression).

Thus, Figures 1 and 2 describe a stable burning process characterized by a constant linear burning rate.

2 Experimental

2.1 Methodology of the experimental determination of the internal ballistic parameters of a solid heterogeneous rocket propellant charge by means of a laboratory rocket motor

Generally, in order to measure the burning rate (r_b) of a solid rocket propellant charge for a given (w_b) and for a given (T_p), utilizing the pressure changes $p(t)$ in the combustion products, obtained during a single combustion process in a LMR (in a single static firing), the following parameters are required:

- the maximum pressure of the combustion products during burning of the tested propellant charge,
- the start time of burning of the tested propellant charge,
- the end time of burning of the tested propellant charge.

Similar methodology has been used worldwide by the leading science and technology centres such as ONERA, SNPE (France), BAYERN-CHEMIE (Germany) and FIAT AVIO (Italy) [4]. Due to this methodology, the time corresponding to 50% of maximum pressure (p_{\max}) on the increasing part of the $p(t)$ curve, was assumed as the start time of burning of the tested propellant charge, and marked as t_1 , and the time corresponding to 50% of (p_{\max}) on the decreasing part of the $p(t)$ curve was assumed as the end time of burning of the tested propellant charge, and marked as t_2 [4, 6]. The resulting burning time (t_b) of the tested propellant charge was determined as:

$$t_b = t_2 - t_1 \quad (6)$$

The values of t_1 , t_2 and t_b were determined from the experimental $p(t)$ relation by means of the *Mathematica*[®] version 8.0.4.0 computational package. Figure 3 presents an example of the pressure $p(t)$ course of combustion products during a single static firing of an SHRP charge in an LRM combustion chamber, with the characteristic time points corresponding to dots lying on the $p(t)$ plot. These points are also necessary for determining the average pressure (p_{av}) of the combustion products in the LRM combustion chamber.

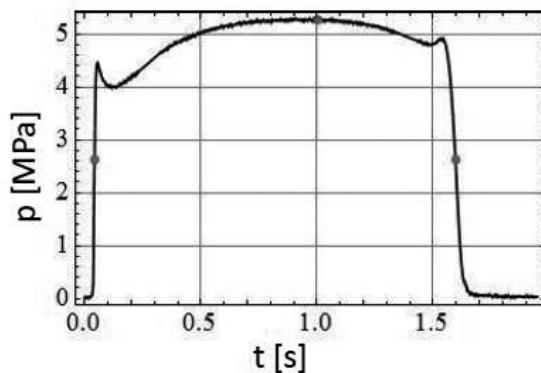


Figure 3. Representative plot of pressure $p(t)$ of the combustion products of the tested SHRP charge during burning, with the characteristic time points t_1 , t_{\max} and t_2 (time coordinates of the pressure respectively).

The burning rate (r_b) for (t_b) was determined from the relation:

$$r_b = w_b/t_b \quad (7)$$

The (p_{av}) of the combustion products during burning in an LRM, for the determined (t_b) obtained from the $p(t)$ curve recorded in a single static firing test (Figure 3), was calculated by means of the following formula:

$$p = p_{av} = \int_{t_1}^{t_2} \frac{p dt}{t_b} \quad (8)$$

2.2 Preparation of the tested solid heterogeneous rocket propellant tubular propellant charges inhibited on the external cylindrical surface

The main components and composition of the SHRP charges tested, of dimensions given in the Introduction, are presented in Table 1.

Bimodal ammonium perchlorate (AP) was used as an oxidiser (small and large sized AP fractions). The weight content of the small sized (fine-grained) AP fraction in the propellant was 21%. The particle diameter of the fine-grained AP fraction was below 60 μm , whilst the particle diameter of the large sized AP fraction was above 60 μm and below 480 μm . The aluminum powder (Al) particle diameter was below 48 μm .

Table 1. Composition of the tested propellant charges.

Ingredients	Content, [wt.%]
Liquid ingredients (α,ω - Dihydroxypolybutadiene prepolymer (HTPB, R45M), Dimeryl Diisocyanate (DDI 1410), Dioctyl adipate, 2,2'-Bis(ethylferrocenyl)propane)	14.75
Aluminum powder	15.00
Ammonium perchlorate	70.00
Additives (bonding agent, antioxidant, surfactant)	0.25

The technological process for obtaining the propellant charges for testing began with the mixing of the propellant ingredients in a Drais planetary mixer of 6 dm³ capacity. The ingredients were added to the mixer in the correct sequence, at an elevated temperature (333 K) and under reduced pressure (5 kPa), and proceeded in accordance with the description given in [6].

The SHRP semi-fluid mass (slurry) was cast into the moulds under reduced pressure. The dimensions of the SHRP charges, including their internal central

channel, were ensured by the utilising identical moulds (4 pcs) with mandrels. Each propellant charge was inhibited on the external cylindrical surface by non-combustible inhibitor jackets inserted into the moulds before filling. Prior to filling the moulds were placed inside a thermostated system with the water jacket temperature at 333 K and the SHRP slurry was then fed into the each mould under a reduced pressure of 5 kPa by means of the filling arrangement shown in Figure 4.



Figure 4. Arrangement for filling the mould with the propellant slurry.

After feeding the appropriate volume of the propellant slurry into the moulds, they were placed in the incubator ($T = 323$ K) and kept there for 5 days in order to obtain sufficiently hardened propellant charges. After hardening, the propellant charges were removed from the moulds and lathe machined to obtain the required dimensions.

The final propellant charges were examined for defects by means of the X-ray radiography method using the HDR (*Hochdynamische Radioskopie*) detector, in order to select charges without any structural defects.

2.3 Laboratory rocket motor – propellant charge configuration and test conditions

To determine (r_b) dependence on (p) of the combustion products of the SHRP charge and the (p) dependence on the (T_p) of the SHRP charge, the special LRM and the method for using this LRM were applied [5, 6] (Figure 5).

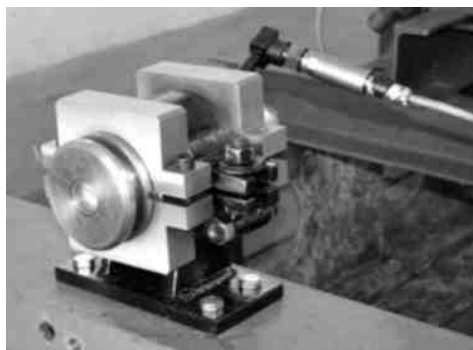


Figure 5. LRM measurement arrangement (static firing test stand).

The measuring system (static firing stand) consisted of the LRM, a tensometric pressure transducer, a MGC Plus digital amplifier and a computer system, allowing the $p = f(t)$ in the LRM combustion chamber, and its dependence on the nozzle critical diameter, to be recorded. The nozzle critical diameters were: 8, 9, 10 and 11 mm. This static firing arrangement allowed the propellant burning rate (utilizing Equation 7) to be determined indirectly.

The SHRP charges inserted into the LRM were conditioned for 6 h at each initial temperature (T_p), viz. 233, 288 or 323 K, before the static firing tests.

The pressure measurements were obtained by means of the tensometric pressure transducers and the MGC Plus digital amplifier. The measurement data were transmitted in *on-line* mode and stored in the computer memory.

2.4 Test results and discussion

From these tests the $p = f(t)$ plots were recorded (see Figures 6-8), with $p(t)$ curves being obtained with nozzles of different critical diameters, viz. 11 (black curve), 10 (the second from the bottom), 9 (the third from the bottom) and 8 (fourth from the bottom) mm; the higher the critical diameter of the nozzle, the lower the average pressure of the combustion products.

On the basis of the recorded $p(t)$ curves (Figures 6-8), and following the indirect methodology described above, values of the time period (t_b), the (p_{av}), the integrals of the temporal pressure calculated for the time period between t_1 and t_2 time points in the burning process, and (r_b), were obtained. These data are collected in Table 2.

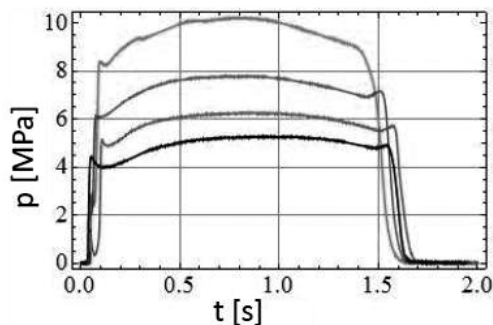


Figure 6. $p = f(t)$ plots for the initial temperature $T_p = 288$ K.

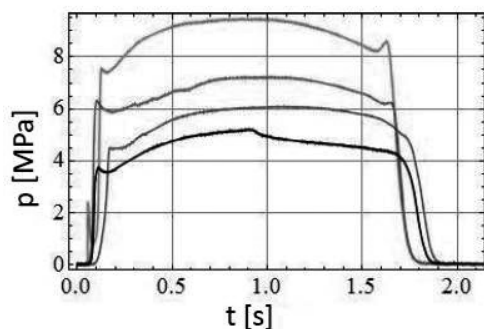


Figure 7. $p = f(t)$ plots for the initial temperature $T_p = 233$ K.

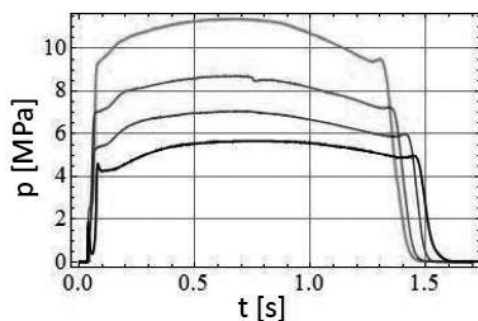


Figure 8. $p = f(t)$ plots for the initial temperature $T_p = 323$ K.

Taking into consideration the dependence of the r_b values on the ratios of the p_{av} and $p_1 = 0.1$ MPa, for an initial temperature of T_p , plots and their mathematical approximation functions were obtained, as shown in Figure 9.

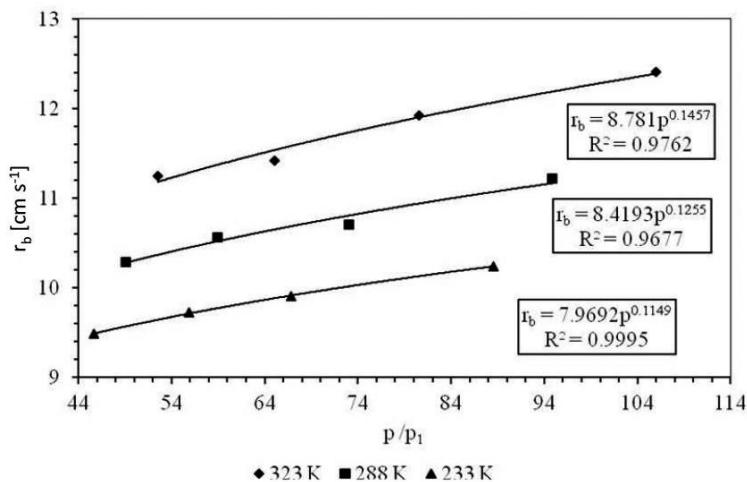


Figure 9. Dependences of $r_b = f(p_{av}/p_1)$ for the three different T_p values.

Taking into consideration the values of the (a) coefficient and its dependence on T_p shown in Figure 9, a plot describing the dependence of (a) on T_p , in approximate form, was obtained (Figure 10).

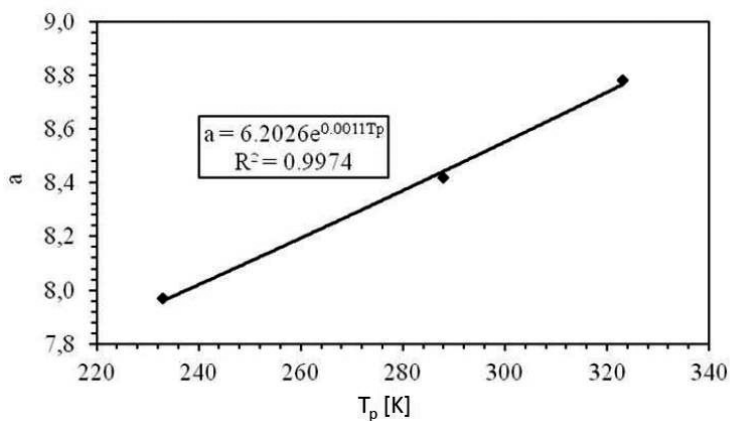


Figure 10. Dependence of the coefficient (a) on the initial temperature (T_p).

Similarly, taking into consideration the values of the (n) coefficient and its dependence on T_p shown in Figure 9, a plot describing the dependence of (n) on T_p , in approximate form, was obtained (Figure 11).

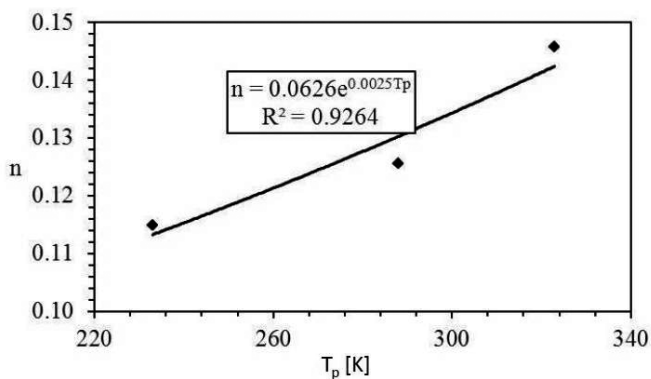


Figure 11. Dependence of the exponent (n) on the initial temperature (T_p).

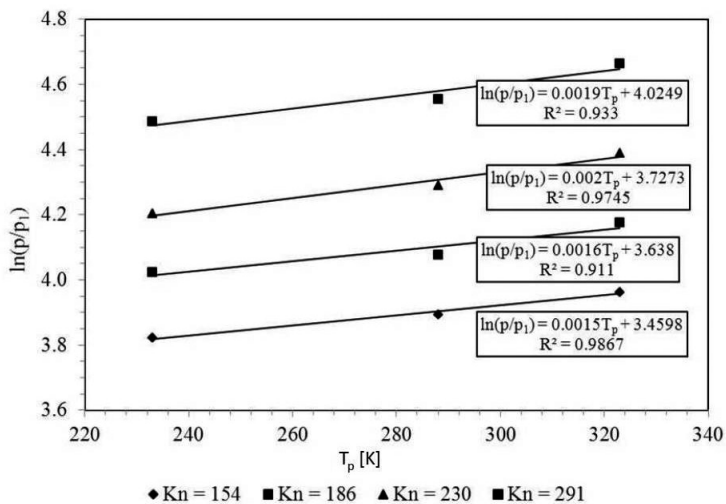


Figure 12. Dependence of $\ln(p/p_1) = f(T_p)$ for the set values of Kn .

For the above three initial temperatures (T_p), the (n) values differ slightly between themselves, their maximum difference being approximately 0.03.

On the basis of Equation (1) and data given in Figures 9-11, it was possible to construct the following experimental dependence of (r_b) on the (p) and on (T_p) for the SHRP charges tested by means of the LRMs:

$$r_b(p, T_p) = a_1 e^{\sigma_p T_p} p^{\vartheta} e^{\sigma_n T_p} = 6.2062 e^{0.0011 T_p} p^{0.0626} e^{0.0025 T_p} \tag{10}$$

where: $a_1 = 6.2062$, $\nu = 0.0626$, $\sigma_n = 0.0025 \text{ K}^{-1}$, and $\sigma_p = 0.0011 \text{ K}^{-1}$.

By comparing Equations (1) and (10), it was found that $a = 6.2062e^{0.0011T_p}$ and $n(p, T_p) = 0.0626e^{0.0025T_p}$. The relationship $\ln(p/p_1) = f(T_p)$ for the given set of Kn values, allowed the π_k values (Figure 12) to be determine. These were as follows: $\pi_k(\text{Kn} = 154) = 0.0015 \text{ K}^{-1}$, $\pi_k(\text{Kn} = 186) = 0.0016 \text{ K}^{-1}$, $\pi_k(\text{Kn} = 230) = 0.002 \text{ K}^{-1}$ and $\pi_k(\text{Kn} = 291) = 0.0019 \text{ K}^{-1}$.

Table 2. Test results

Item	Experiment No.	Initial temp. [K]	p_{\max}	t_b	$\int_{t_1}^{t_2} p dt$	p_{av}	Nozzle critical diameter	w_b	r_b [mm/s]
			[MPa]	[s]	[MPa·s]	[MPa]	[mm]		
1	62	323	5.69	1.422	7.48	5.26	11.00	16.0	11.25
2	63		7.08	1.401	9.11	6.50	10.00	16.0	11.42
3	64		8.72	1.342	10.80	8.05	9.00	16.0	11.92
4	65		11.38	1.289	13.66	10.60	8.00	16.0	12.41
1	54	288	5.28	1.556	7.63	4.91	11.00	16.0	10.28
2	55		6.28	1.515	8.92	5.89	10.00	16.0	10.56
3	56		7.79	1.495	10.91	7.30	9.00	16.0	10.70
4	57		10.22	1.427	13.53	9.49	8.00	16.0	11.21
1	58	233	5.21	1.687	7.71	4.57	11.00	16.0	9.48
2	59		6.09	1.646	9.20	5.59	10.00	16.0	9.72
3	60		7.23	1.615	10.80	6.69	9.00	16.0	9.91
4	61		9.46	1.563	13.84	8.86	8.00	16.0	10.24

3 Conclusions

The LRM and its measurement method enabled the following internal ballistic characteristics of the SHRP charges to be determined indirectly:

- the dependence of the burning rate (r_b) on the pressure (p) and on the initial temperature (T_p), which corresponds closely to the actual conditions that occur in full-scale rocket motors,
- the sensitivity coefficient (n) of (r_b) to (p), the sensitivity coefficient (σ_p) of (r_b) to (T_p), and the sensitivity coefficient (π_k) of (p) of the combustion products to (T_p).

The sensitivity coefficient (π_k) of the pressure to (T_p) for the SHRPs tested, changed from 0.0015 to 0.0020 K^{-1} , increasing slightly with increase in Kn.

Generally, the SHRP charges tested were characterized by low sensitivity

coefficients (n), σ_p , π_k . These low sensitivity coefficients indicate low sensitivity of these SHRP charges to pressure and temperature changes.

The tests enabled the experimental dependence of (r_b) on the combustion products pressure (p) and on (T_p) to be determined in the general form given in mathematical formula (10).

Acknowledgements

The work was supported by the Polish Ministry of Science and Higher Education from 2010-2013 funds, as research project No. O R00 0090 09.

4 References

- [1] Kubota N., *Propellants and Explosives. Thermochemical Aspects of Combustion*, Wiley-VCH GmbH, Weinheim, **2007**, pp.17, 412.
- [2] Maggi F., DeLuca L.T., Bandera A., Burn-rate Measurement on Small-scale Rocket Motors, *Def. Sci. J.*, **2006**, *56*, 353-367.
- [3] Strecker R., Ch. 3, *Comparison of Burning Rate Measurements Technologies/ Devices*, NATO-RTO Technical Report No. RTO-TR-043, **2002**, 38.
- [4] Fry R.S., Gadiot G.M.H.J.L., Ch. 4, *Burning Rate Measurement Analysis Method*, NATO-RTO Technical Report No. RTO-TR-043, **2002**, (Table 4.6), 62.
- [5] Florczak B., Białek M., Szczepanik M., Dzik A., Studies on Elaborating Non-homogeneous Solid Rocket Propellant for Propellant Cartridges Bonded to Motor Chamber Well, *Chemik*, **2013**, *67*(1), 25-32.
- [6] Florczak B., Białek M., Szczepanik M., Dzik A., Matłok A., Study on Double-base Propellant with Laboratory Rocket Motor (in Polish), *Przem. Chem.*, **2013**, *92*(6), 1042-1045.
- [7] Florczak B., Investigation of an Aluminized Binder/AP Composite Propellant Containing FOX-7, *Cent. Eur. J. Energ. Mater.*, **2008**, *5*(3-4), 65-75.
- [8] Florczak B., Kwilosz S., Cholewiak A., Białek M., Miszczak M., *Laboratory Rocket Motor* (in Polish), PL Patent 217675, **2014**.

